Applied Microscopy
Korean Society of Microscopy
pISSN 2287-5123 · eISSN 2287-4445
http://dx.doi.org/10.9729/AM.2015.45.1.32
Regular Article

Microstructural Features of Multicomponent $FeCoCrNiSi_x$ Alloys

Kyeong Ho Kong, Kang Cheol Kim, Won Tae Kim[1], Do Hyang Kim*

Center for Non-crystalline Materials, Department of Materials Science and Engineering, Yonsei University, Seoul 120-749, Korea
[1]Department of Optical Engineering, Cheongju University, Cheongju 363-764, Korea

*Correspondence to:
Kim DH,
Tel: +82-2-2123-4254
Fax: +82-2-312-8281
E-mail: dohkim@yonsei.ac.kr

Received March 24, 2015
Revised March 26, 2015
Accepted March 26, 2015

The microstructural features of FeCoCrNi, FeCoCrNiAl and $FeCoCrNiSi_x$ (x=0, 5, 10, 15, 20) alloys have been investigated in the present study. The microstructure of FeCoCrNi alloy changes dramatically with equiatomic addition of Al. The fcc irregular shaped grain structure in the as-cast FeCoCrNi alloy changes into the bcc interconnected structure with phase separation of Al-Ni rich and Cr-Fe rich phases in the as-cast FeCoCrNiAl alloy. The microstructure of FeCoCrNi alloy changes with the addition of Si. With increasing the amount of Si, the fcc structure of the grains is maintained, but new phase containing higher amount of Si forms at the grain boundary. As the amount of Si increases, the fraction the Si-rich grain boundary phase increases.

Key Words: High entropy alloy, FeCoCrNi alloy, Solid solution, Si addition

INTRODUCTION

Recently, one of the new types of multicomponent alloys, high entropy alloy with major alloying elements in equiatomic or near-equiatomic ratios, receives a great attention as a new potential alloys due to their unique microstructural features and outstanding properties (Ranganathan, 2003; Cantor et al., 2004; Hsu et al., 2004; Huang et al., 2004; Yeh et al., 2004). The most eminent property enhancement including wear resistance, corrosion resistance, oxidation resistance and hardness has been reported previously (Chen et al., 2004; Huang et al., 2004; Chen et al., 2005; Wu et al., 2006). These findings have brought new insight in design of alloys when compared with the alloys which are currently being developed, and has provided a new concept in designing of modern alloys. As a result, a series of new multicomponent systems has been investigated (Wang & Zhang, 2008). Among the alloying elements available for new alloy design, Fe, Co, Ni, Ti, Cu, and Al have been used most frequently to synthesize the high entropy alloys. Among the alloying elements which have been mostly used, Fe, Co, Ni, Ti, Cu are transition metal elements. It has been shown that the addition of small amount of alloying element can occasionally induce a dramatic property enhancement in traditional alloys (Itabashi & Kawata, 2000; Lin & Chang, 2003; Kondo & Takahashi, 2006). While there are quite few reports on the effect of alloying element such as Si with small atomic radius on the microstructure development and property enhancement in high entropy alloys. Therefore, the aim of the present study is to investigate the effect of addition of alloying elements Al, Si on the microstructural development in FeCoCrNi high entropy alloys. The addition of Al in FeCoCrNi high entropy alloy has been reported to cause the change of the crystal structure of solid solution from fcc to bcc (Wang et al., 2012). In the present study, effect of Al addition has been investigated to confirm the previous result. Then, the effects of Si addition on the microstructural development in FeCoCrNi high entropy alloy has been investigated systematically. The result shows that the addition of Si element changes the alloy structure evidently, which further provides the potential for improvement of properties.

This work was supported by the Global Research Laboratory Program of the Korean Ministry of Education, Science and Technology.

MATERIALS AND METHODS

The FeCoCrNi, FeCoCrNiAl, and $FeCoCrNiSi_x$ (x=0, 5, 10, 15, 20) alloy ingots were alloyed from high-purity elements using arc melting in water-cooled molds under argon atmosphere. The ingots were re-melted at least three times to improve their chemical homogeneity. The nominal chemical compositions are listed in Table 1. The alloy ingots were re-melted, and poured into the cylinder-type molds with the diameter of 2 and 5 mm. The microstructure of the specimens wase compared after polishing and etching. The specimens were observed under a scanning electron microscope (SEM, JSM-7001F; JEOL, Japan). The chemical composition of the phases in these alloys was analyzed by energy dispersive spectrometry (EDS, 51-ADD0069; Oxford Instruments, UK) assembled in SEM. X-ray diffractometer (XRD, Ultima IV; Rigaku, Japan) with Cu K_α radiation for a 2θ range of 30° to 80° at a speed of 4°/min was used for identification of the crystalline structures in the alloys.

Table 1. Chemical compositions of the alloys investigated in the present study (at%)

Alloy	Al	Co	Cr	Fe	Ni	Si
CoCrFeNi	-	25	25	25	25	-
AlCoCrFeNi	20	20	20	20	20	-
$CoCrFeNiSi_5$	-	23.75	23.75	23.75	23.75	5
$CoCrFeNiSi_{10}$	-	22.5	22.5	22.5	22.5	10
$CoCrFeNiSi_{15}$	-	21.25	21.25	21.25	21.25	15
$CoCrFeNiSi_{20}$	-	20	20	20	20	20

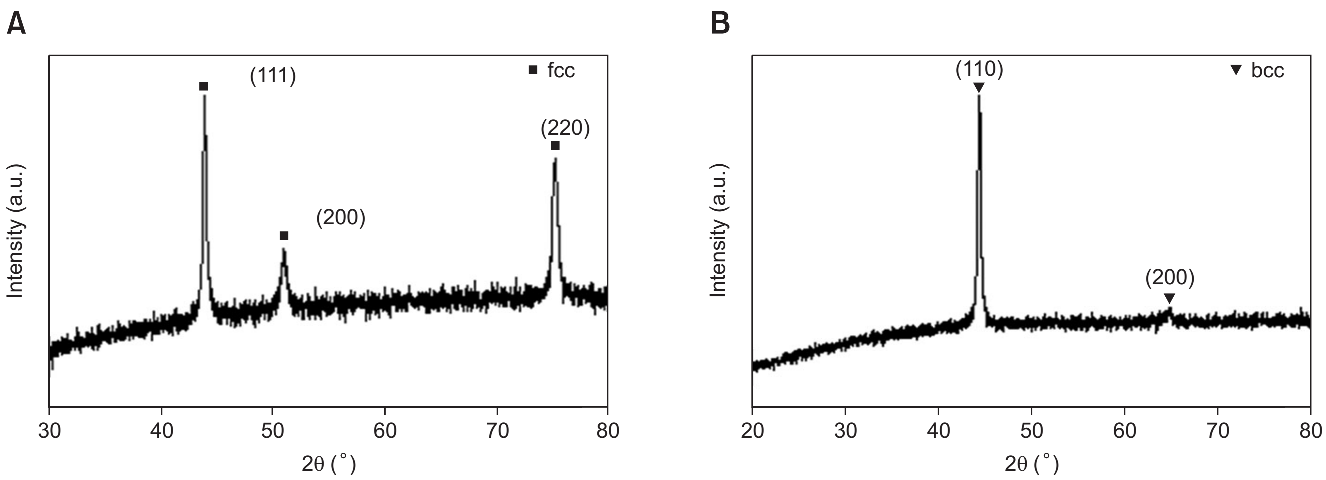

Fig. 1. X-ray diffractometer patterns obtained from the as-cast FeCoCrNi (A) and FeCoCrNiAl (B) alloys.

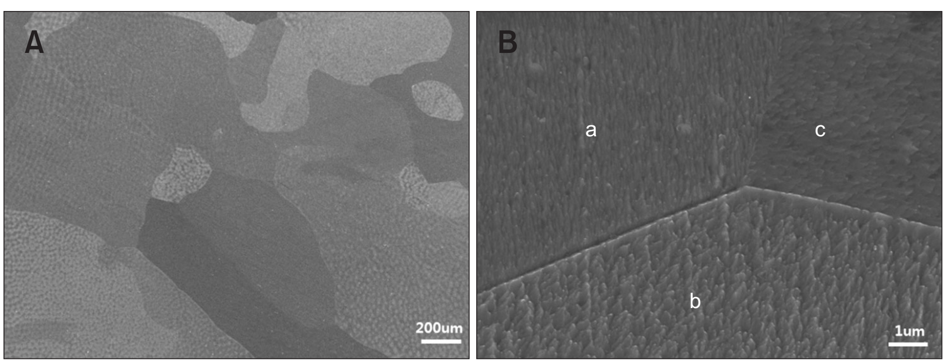

Element	a (at%)	b (at%)	c (at%)
Cr	26.39	26.42	26.26
Fe	23.65	23.24	24.39
Co	25.69	25.78	23.61
Ni	24.29	24.55	25.74

Fig. 2. Scanning electron microscope images with low (A) and high (B) magnification obtained from the as-cast FeCoCrNi alloy. Energy dispersive spectrometry results obtained from the area marked 'a', 'b', and 'c' in Fig. 2B.

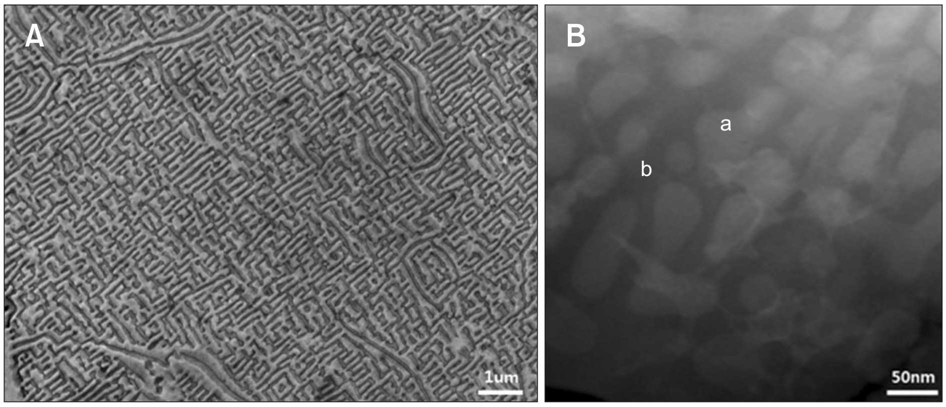

Element	a (at%)	b (at%)
Al	1.76	30.94
Cr	47.46	11.84
Fe	27.45	15.09
Co	17.51	19.64
Ni	5.82	22.49

Fig. 3. Scanning electron microscope images with low (A) and high (B) magnification obtained from the as-cast FeCoCrNiAl alloy. Energy dispersive spectrometry results obtained from the area marked 'a' and 'b' in Fig. 3B.

RESULTS AND DISCUSSION

Effect of Al Addition in FeCoCrNi Alloy

Fig. 1 shows the XRD patterns obtained from the as-cast FeCoCrNi and FeCoCrNiAl alloys (diameter, 2 mm). The diffraction peaks from the as-cast FeCoCrNi alloy were identified as a single fcc phase with the lattice parameter of 0.357 nm, while those form the as-cast FeCoCrNiAl alloy were identified as a single bcc phase with the lattice parameter of 0.287 nm. Fig. 2 shows the low and high magnification SEM images obtained from the as-cast FeCoCrNi alloy together with the EDS results taken from the area marked 'a', 'b', and 'c' in Fig. 2B. From the SEM image in Fig. 2A, the as-cast FeCoCrNi alloy consisted of irregular-shaped grains without any secondary solidification phase. The composition of the grains marked 'a', 'b', and 'c' in Fig. 2B were 26.4% Cr-23.7% Fe-25.7% Co-24.3% Ni, 26.4% Cr-23.2% Fe-25.8% Co-24.6% Ni, and 26.3% Cr-24.4% Fe-23.6% Co-25.7% Ni, respectively (hereafter, the composition is in at%), indicating that the composition is almost homogeneous throughout the whole grains. On the other hand, the as-cast FeCoCrNiAl alloy exhibited a very much different microstructure, as can be seen from the low magnification SEM image in Fig. 3A. The microstructure consisted of a very complicated interconnected structure, indicating that phase separation occurred during solidification. The EDS results obtained from the regions marked 'a' and 'b' in Fig. 3B show that the compositions after phase separation were 1.76% Al-47.5% Cr-27.5% Fe-17.5% Co-5.82% Ni and 30.9% Al-11.84% Cr-15.1% Fe-19.6% Co-22.5% Ni, respectively. The result indicates that the phase separation occurred into Al-Ni rich and Cr-Fe rich phases. The result in Fig. 1-3 suggest that the

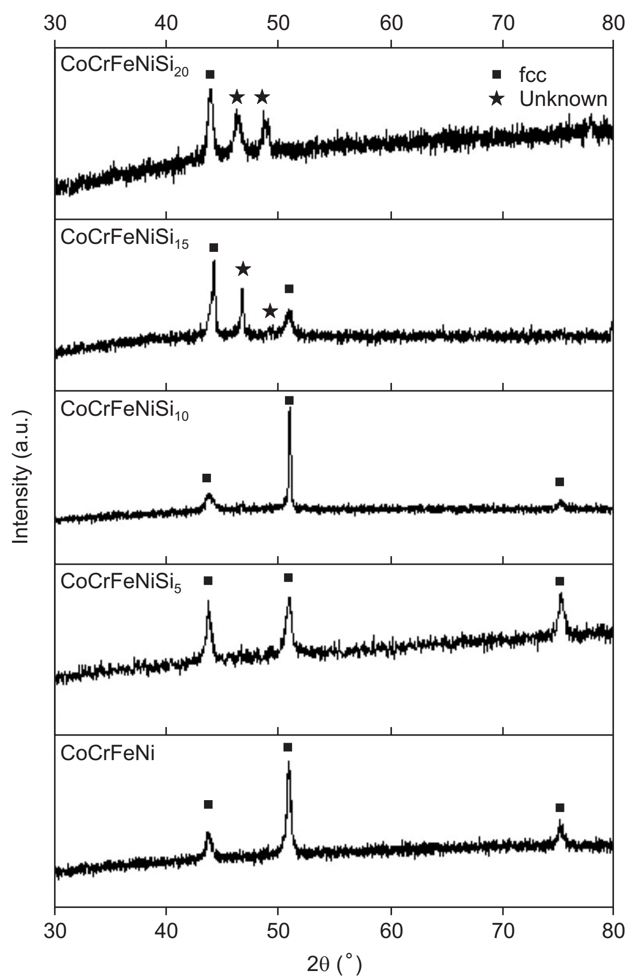

Fig. 4. X-ray diffractometer patterns obtained from the as-cast $FeCoCrNiSi_x$ (x=0, 5, 10, 15, 20) alloys.

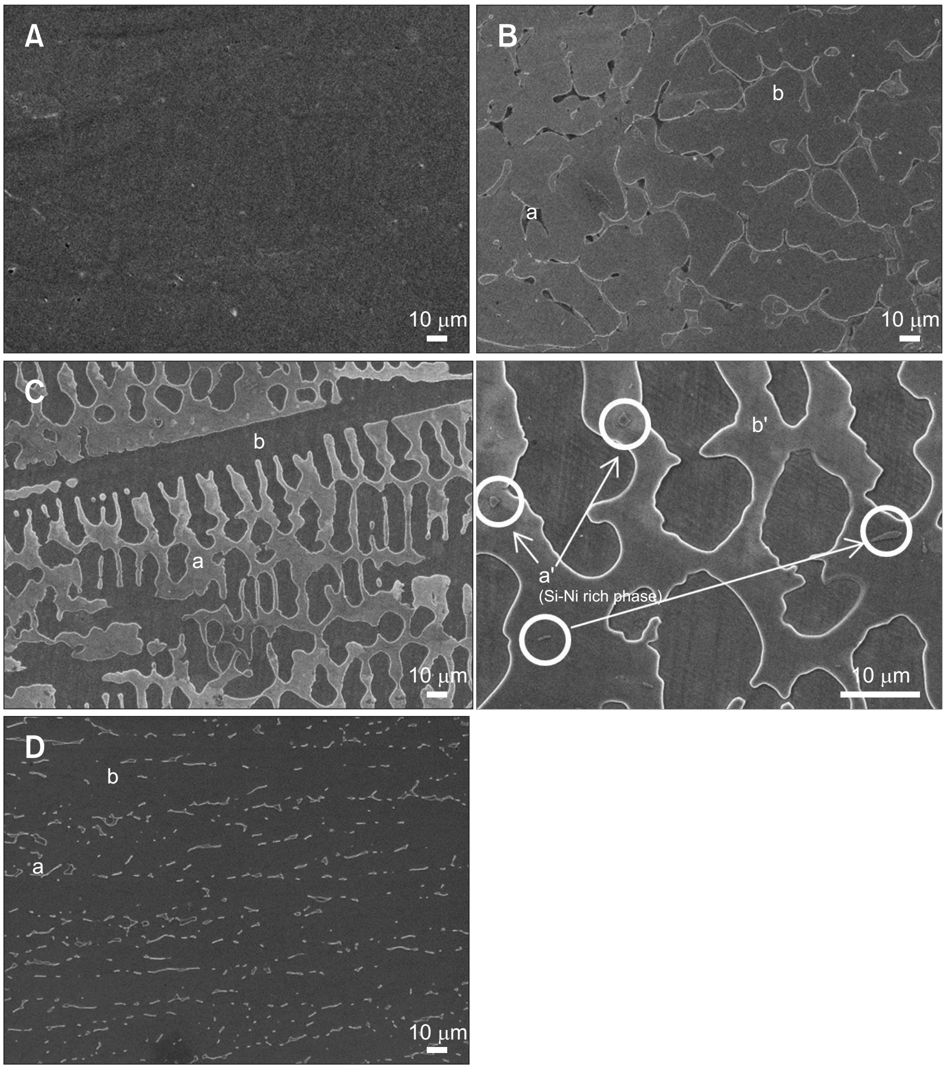

Fig. 5. Scanning electron microscope image obtained from the as-cast $FeCoCrNiSi_x$ alloys: (A) x=5%; (B) x=10%; (C) x=15%; and (D) x=20%. EDS results obtained from the area marked in Fig. 5.

microstructure of FeCoCrNi alloy changes dramatically with equiatomic addition of Al. In other words, the fcc irregular shaped grain structure with homogeneous composition distribution changes into the bcc interconnected structure with phase separation forming Al-Ni rich and Cr-Fe rich phases.

Effect of Si Addition in FeCoCrNi Alloy

Fig. 4 compares the XRD patterns obtained from the as-cast $FeCoCrNiSi_x$ (x=0, 5, 10, 15, 20) alloys (diameter, 2 mm). As mentioned above, the as-cast FeCoCrNi alloy consisted of a single solid solution with the fcc structure. With addition of 5% and 10% of Si, the alloy still consisted of the fcc structure, as can be seen from the diffraction peaks in Fig. 4. However, with addition of 15% and 20%, the diffraction peaks from the fcc structure still remained, but new diffraction peaks from the other phase appeared, as can be seen in Fig. 4. Fig. 5A shows the SEM image obtained from the as-cast FeCoCrNiSi5 alloy. The microstructure was almost same as that of alloy without Si shown in Fig. 2. The compositions measured by EDS from the area marked in Fig. 5 are listed in Table 2. The composition of the solid solution was 5.0% Si-24.0% Cr-25.2% Fe-23.7% Co-22.1% Ni, indicating that Si was homogeneously distributed in the grains. When higher amount of Si, 10% was added in the FeCoCrNi alloy, new phase began to form at the grain boundary of the fcc grains, as can be seen in Fig. 5B. The composition measured from the regions from 'a' and 'b' in Fig. 5B were 22.4% Si-19.4% Cr-16.1% Fe-16.2% Co-26.1% Ni and 10.8% Si-24.6% Cr-22.8% Fe-21.5% Co-20.4% Ni, respectively. The result shows that Si was enriched in the phase formed at the grain boundaries. The crystal structure of the Si-rich phase could not be determined in the present study. When the Si content was further increased up to 15%, the fraction of Si-rich phase increased significantly, as can be seen in Fig. 5C. The compositions measured from the regions from 'a' and 'b' in

Table 2. Energy dispersive spectrometry results* (at%)

Element	Si	Cr	Fe	Co	Ni
$FeCoCrNiSi_5$					
Grain	5.0	24.0	25.2	23.7	22.1
$FeCoCrNiSi_{10}$					
a	22.4	19.4	16.1	16.2	26.1
b	10.8	24.6	22.8	21.5	20.4
$FeCoCrNiSi_{15}$					
a	24.3	19.5	15.8	17.9	22.5
b	13.1	22.4	23.4	22.3	18.9
a'	27.7	8.7	10.3	16.3	37.0
b'	25.0	17.2	17.3	17.4	23.2
$FeCoCrNiSi_{20}$					
a	29.5	8.5	13.3	18.8	30.0
b	21.9	20.9	19.6	18.4	19.2

*The results obtained from the area marked in Fig. 5.

Fig. 5C were 24.3% Si-19.5% Cr-15.8% Fe-17.9% Co-22.5% Ni and 13.1% Si-22.4% Cr-23.4% Fe-22.3% Co-18.9% Ni, respectively. The compositions of the Si-rich grain boundary phase and the fcc structure grain were almost same as those in the alloy containing 5% Si. However, it can be noticed that Si-Ni rich phase (27.7% Si-8.7% Cr-10.3% Fe-16.3% Co-37.0% Ni) is newly formed in the Si-rich phase. When Si content was 20%, the microstructure mostly consisted of Si-Ni rich phase. The result in Fig. 4 and 5 indicates that the microstructure of FeCoCrNi alloy changes dramatically with the addition of Si. With increasing the amount of Si, the fcc structure of the grains is maintained, but new phase containing higher amount of Si forms at the grain boundary. As the amount of Si increases, the fraction the Si-rich grain boundary phase increases.

CONCLUSIONS

In the study, the microstructural features of FeCoCrNi, FeCoCrNiAl, and $FeCoCrNiSi_x$ (x=0, 5, 10, 15, 20) alloys have been investigated. The main conclusions are as follows: (1) The microstructure of FeCoCrNi alloy changes dramatically with equiatomic addition of Al. The fcc irregular shaped grain structure with homogeneous composition distribution in the as-cast FeCoCrNi alloy changes into the bcc interconnected structure with phase separation forming Al-Ni rich and Cr-Fe rich phases in the as-cast FeCoCrNiAl alloy. (2) The microstructure of FeCoCrNi alloy changes with the addition of Si. With increasing the amount of Si, the fcc structure of the grains is maintained, but new phase containing higher amount of Si forms at the grain boundary. As the amount of Si increases, the fraction the Si-rich grain boundary phase increases.

CONFLICT OF INTEREST

No potential conflict of interest relevant to this article was reported.

REFERENCES

Cantor B, Chang I T H, Knight P, and Vincent A J B (2004) Microstructural development in equiatomic multicomponent alloys. *Mater. Sci. Eng. A* **375**, 213-218.

Chen T K, Shun T T, Yeh J W, and Wong M S (2004) Nanostructured nitride films of multi-element high-entropy alloys by reactive DC sputtering. *Surf. Coat. Technol.* **188-189**, 193-200.

Chen Y Y, Duval T, Hung U D, Yeh J W, and Shih H C (2005) Microstructure and electrochemical properties of high entropy alloys- a comparison with type-304 stainless steel. *Corr. Sci.* **47**, 2257-2279.

Hsu C Y, Yeh J W, Chen S K, and Shun T T (2004) Wear resistance and high-temperature compression strength of fcc CuCoNiCrAl0.5Fe alloy with boron addition. *Metall. Mater. Trans. A* **35**, 1465-1469.

Huang P K, Yeh J W, Shun T T, and Chen S K (2004) Multi-principal-element alloys with improved oxidation and wear resistance for thermal spray coating. *Adv. Eng. Mater.* **6**, 74-78.

Itabashi M and Kawata K (2000) Carbon content effect on high-strain-rate tensile properties for carbon steels. *Int. J. Impact Eng.* **24**, 117-131.

Kondo M and Takahashi M (2006) Corrosion resistance of Si- and Al-rich steels in flowing lead-bismuth. *J. Nucl. Mater.* **356**, 203-212.

Lin D Y and Chang T C (2003) Influence of Si content on the intergranular corrosion of SUS 309L stainless steels. *Mater. Sci. Eng. A* **359**, 396-401.

Ranganathan S (2003) Alloyed pleasures: multimetallic cocktails. *Curr. Sci.* **85**, 1404-1406.

Wang F J and Zhang Y (2008) Effect of Co addition on crystal structure and mechanical properties of Ti0.5CrFeNiAlCo high entropy alloy. *Mater. Sci. Eng. A* **496**, 214-216.

Wang W R, Wang W L, Wang S C, Tsai Y C, Lai C H, and Yeh J W (2012) Effects of Al addition on the microstructure and mechanical property of AlxCoCrFeNi high-entropy alloys. *Intermetallics* **26**, 44-51.

Wu J M, Lin S J, Yeh J W, Chen S K, Huang Y S, and Cheng H C (2006) Adhesive wear behavior of AlxCoCrCuFeNi high-entropy alloys as a function of aluminum content. *Wear* **261**, 513-519.

Yeh J W, Chen S K, Lin S J, Gan J Y, Chin T S, Shun T T, Tsau C H, and Chang S Y (2004) Nanostructured high-entropy alloys with multiple principal elements: novel alloy design concepts and outcomes. *Adv. Eng. Mater.* **6**, 299-303.